

Characteristics of Coal Dust Deposition in Boiler Tail Gas Pipelines

Hui quan Liu^{1,2}, Yu Wang^{1,2}, and Hao Lu^{1,2,3*}

¹School of Electrical Engineering, Xinjiang University, 830047 Urumqi, China

²Laboratory of Energy Carbon Neutrality, School of Electrical Engineering, Xinjiang University, 830047 Urumqi, China

³Center of New Energy Research, School of Future Technology, Xinjiang University, 830047 Urumqi, China

Abstract. Coal dust deposition in boiler tail gas pipelines can significantly affect boilers' thermal and energy efficiency. This study investigates the deposition characteristics of coal dust particles in boiler tail gas tubes in variable cross-section tubes. Numerical simulations were performed using the Reynolds Stress Model and the Discrete Particle Model. User-defined functions coding is used to construct the particle deposition model in the particle deposition model. The study analyses the distribution of turbulent kinetic energy locations in the gradient tube, compares the distribution of particle deposition on its wall, and concludes that the deposition distribution of coal dust particles in the gradient tube is slightly different for different particle sizes. Smaller particles have a higher deposition efficiency in equal cross-section pipes than larger particles. Particle size also has a significant effect on pipe taper and expansion. The results of this study can provide theoretical guidance for optimising the design of boiler tail gas pipelines, improving energy efficiency, and reducing environmental pollution.

1 Introduction

China is the world's largest producer and consumer of coal[1]. As an essential part of China's energy sector, coal accounts for about 60% of total energy consumption and is critical in guaranteeing China's energy supply and security[2, 3]. After Xi Jinping presented the twin carbon targets of "peak carbon" and "carbon neutral" at the 75th UN General Assembly in September 2020, China formally joined the low-carbon energy system transition strategy, which is centred on the replacement of fossil fuels with cleaner energy sources and renewable energy[4]. Therefore, research on the clean utilisation of coal in the boiler combustion process is an imminent problem.

Boiler exhaust emissions during boiler combustion are a common environmental problem in industrial production. With the acceleration of industrialisation and the growth of energy demand, coal-fired boilers have become one of the significant energy conversion devices and play an essential role in energy production and utilisation. However, solid particulate matter (PM) emitted from boiler exhaust, considered a primary hazardous substance, especially coal dust particulate matter, severely impacts the environment and public health[5]. Coal dust particulate matter deposited on the pipe surface in the pipeline will reduce the heat transfer efficiency between the inside of the pipe and the outside environment, leading to poor heat transfer in the discharge pipe, thus affecting the temperature distribution of the flue gases, which in turn affects the thermal efficiency of the boiler and the efficiency of

energy utilisation. In addition, particles will erode the wall surface, thus reducing the pipeline's service life. In severe cases, even clogging will occur, seriously threatening the stability and safety of the heat exchange system operation. Moreover, particulate matter causes atmospheric pollution and may pollute the delicate particulate matter (PM_{2.5}) in the atmosphere, affecting air quality and increasing the incidence of respiratory diseases. Therefore, a thorough investigation of the deposition characteristics of pulverised coal particulate matter in boiler tail gas pipes is required to improve the operating economy and efficiency of the relevant equipment.

With the rapid development of Computational Fluid Dynamics (CFD), researchers have had significant success in studying particle deposition in channel flows. Li et al. [6] pioneered using the Eulerian-Eulerian model to compute the particle deposition problem. They found that it has the same accuracy as the Lagrangian method and uses fewer computational resources. Jiang et al. [7] simulated the deposition of particles in rectangular channels made of different materials. They found a significant correlation between the dimensionless deposition rate of particles and the physical properties of the channel wall. This study highlighted the importance of taking into account the variation in wall physical properties. Xu et al. [8] simulated the deposition of particles in ventilation ducts under the same operating conditions using both the Lagrangian and Eulerian methods and showed that the latter is less computationally expensive, and is, therefore, more suitable for engineering applications that require larger

* Corresponding author: luhao@xju.edu.cn

computational resources. Yao et al. [9] explored the effect of several important parameters in the viscosity model on the Eulerian simulation, and they concluded that the Eulerian multiphase flow model using the proposed fluid approach can be used for a wide range of applications. Lu et al. [10] utilized numerical simulations with RSM and DPM coupling to investigate turbulence conditions and particle deposition in a straight pipe with a variable cross-section. Yang et al. [11] developed a dynamic CFD model based on inertial collisions, thermophoretic forces, and direct condensation of alkaline vapor. The concept of collision efficiency was introduced, which can effectively analyze the variation of particle size deposition with velocity. Han et al. [12] employed the Eulerian-Eulerian CFD approach to forecasting the deposition of particles in pipelines after comparing it with asphalt scaling experiments and finding that the two were in good agreement. Vargas et al. [13] predicted a two-dimensional particle transport process using the Eulerian model, which was compared favourably to experimental findings and showed good accuracy.

Although existing studies have focussed on particulate emission and capture technologies, the deposition characteristics of coal dust particulate matter in boiler tail gas ducts are still not well understood. In this study, the deposition characteristics of coal dust particulate matter in variable cross-section pipelines are systematically investigated by numerical simulation, and the relationship between the particulate matter deposition and the pipeline structure, operating parameters, and other factors are discussed. This research provides valuable insights into optimizing the design of boiler tail gas pipelines to improve energy efficiency and reduce environmental pollution.

The article is structured as follows: the introduction describes the background and significance of the study; the second section describes the numerical method, including the fluid phase and particle phase models; the third section discusses the selection of the physical model and the computational mesh; the fourth section presents and analyses the simulation results, including the flow characteristics and particulate matter deposition characteristics; and the fifth section summarises the findings and suggests directions for future research.

2 Numerical methods

2.1 Fluid Phase Models

The flow of a fluid in a pipe must obey the equation of continuity, the equation of momentum, and the equation of energy, which are given as follows.:

$$\frac{\partial \bar{\rho} u_i}{\partial x_i} = 0 \quad (1)$$

$$\frac{\partial \bar{u}_i}{\partial t} + \bar{u}_j \frac{\partial \bar{u}_i}{\partial x_j} = -\frac{1}{\rho} \frac{\partial \bar{p}}{\partial x_i} + \frac{1}{\rho} \frac{\partial}{\partial x_j} \left(\mu \frac{\partial \bar{u}_i}{\partial x_j} - \rho \bar{u}_i \bar{u}_j \right) \quad (2)$$

$$\frac{\partial T}{\partial t} + \frac{\partial}{\partial x_i} (\bar{u}_i T) = \frac{\partial}{\partial x_i} \left(\frac{\lambda}{\rho c_p} \frac{\partial T}{\partial x_i} \right) \quad (3)$$

The RSM model is a more complex and refined one derived by Gibson and Launder[14], which considers the various anisotropies in the flow process and allows for better secondary flow simulation. Tian and Ahmadi[15] studied particle deposition in a straight pipe using different turbulence models. They found that the Reynolds stress model (RSM) is suitable for measuring particle deposition compared to other turbulence models. Haibullina et al. [16] concluded that the RSM with enhanced wall treatment can effectively predict the time-averaged flow field. After size analysis and finishing, the Reynolds stress equation is written as follows:

$$\frac{\partial}{\partial t} (\bar{u}_i \bar{u}_j) + \bar{u}_k \frac{\partial}{\partial x_k} (\bar{u}_i \bar{u}_j) = \underbrace{\frac{\partial}{\partial x_k} \left(\frac{\nu_t}{\sigma_k} \frac{\partial \bar{u}_i \bar{u}_j}{\partial x_k} \right)}_{D_{T,ij} = \text{TurbulentDif fusion}} - \underbrace{\left(\bar{u}_i \bar{u}_k \frac{\partial \bar{u}_j}{\partial x_k} + \bar{u}_j \bar{u}_k \frac{\partial \bar{u}_i}{\partial x_k} \right)}_{P_{ij} = \text{StressProduction}} - C_1 \frac{\varepsilon}{k} \left[\bar{u}_i \bar{u}_j - \frac{2}{3} \delta_{ij} k \right] - C_2 \left[P_{ij} - \frac{2}{3} \delta_{ij} P \right] - \frac{2}{3} \delta_{ij} \varepsilon \quad (4)$$

$\phi_{ij} = \text{Pressurestrain}$

In this study, to ensure that the fluid is in a fully developed state in the pipe, Fluent User-defined functions (UDF) will be used at the inlet of the fluid to define the flow velocity distribution at the inlet. The more used power of the seven laws[17] is used in this study and is given below:

$$U = U_{free} \left(\frac{y}{H/2} \right)^{1/7} \quad \text{for } y \leq H/2 \quad (5)$$

$$U = U_{free} \left(\frac{H-y}{H/2} \right)^{1/7} \quad \text{for } y > H/2 \quad (6)$$

$$U_{free} = \frac{8}{7} U_{mean} \quad (7)$$

where U_{mean} is the average fluid velocity at the inlet and the pipe's height.

2.2 Particle phase models

The discrete phase method (DPM) calculates the particle phase. By computing the balance of forces acting on the particles, the trajectory of the particles may be predicted. Due to the low mass loading of the particles, single-phase coupling is used to perform the particle phase calculations without considering the collision and rotation between the particles. In the previous study[18], we consider drag, gravity, buoyancy, Brownian force, heat flow, and Saffman lift force to calculate the particle forces. The equations are as follows:

$$m_p \frac{du_p}{dt} = F_D + F_G + F_B + F_S + F_T \quad (8)$$

Where F_D , F_G , F_B , F_S , F_T is the trailing, gravitational, Brownian, Saffman lift, and thermophoretic forces on the particles.

$$F_D = \frac{1}{\tau_p} \frac{C_D Re_p}{24} (u_g - u_p) \quad (9)$$

In the traction equation, u_g , u_p represents the fluid and particle velocities, respectively. C_D is the drag coefficient, and τ_p is the relaxation time of the particles, calculated as:

$$C_D = \begin{cases} \frac{24}{Re_p}, & \text{for } Re_p < 1 \\ \frac{24}{Re_p} (1 + 0.15 Re_p^{0.687}), & \text{for } 1 < Re_p < 400 \end{cases} \quad (10)$$

$$\tau_p = \frac{S d_p^2 C_C}{18\nu} \quad (11)$$

$$C_C = 1 + \frac{2\lambda}{d_p} \left(1.257 + 0.4e^{-(1.1d_p/2\lambda)} \right) \quad (12)$$

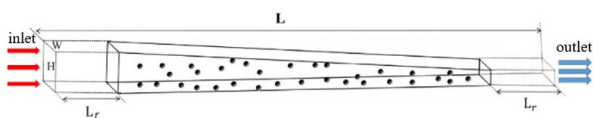
$$Re_p = \frac{d_p (u_g - u_p)}{\nu} \quad (13)$$

Where S is the particle-to-fluid density ratio, ν is the kinematic viscosity, d_p is the particle size, and C_C is the Cunningham slip correction factor. Where λ is the mean free range of gas molecules, $0.065 \mu m$ at $25^\circ C$ and atmospheric pressure, and Re_p is the relative Reynolds number.

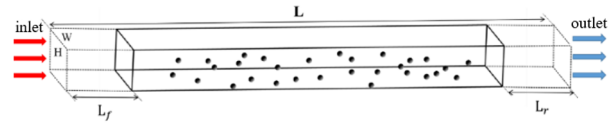
3 Physical Models and Computational Grids

In this study, the particle deposition characteristics in variable cross-section pipes are investigated based on standard pipes in the engineering field, using a simplified physical model and structured grid as shown in Figures 1 and 2. The length of the straight pipe section is 900 mm, and the cross-section is a rectangle with a width-to-height ratio of 2:1. To ensure full development of the fluid flow state in the pipe, a development section was added at the front end of the pipe and an extension section was added at the back end to minimize the effect of the exit backflow. Particulate matter is released from the inlet and deposited on the pipe wall.

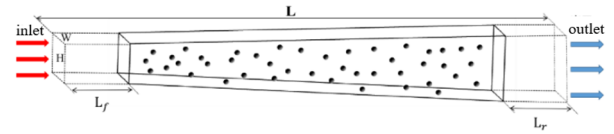
For the simulation, we chose the RSM turbulence model for the fluid phase simulation and used the DPM model for the particulate phase simulation. The RSM turbulence model was used to capture the complex turbulence characteristics, while the DPM model was used to simulate the particulate movement and deposition process. A fully developed velocity profile is imposed at the inlet through the DEFINE_PROFILE macro in Fluent, which uses the seventh power law to ensure that the velocity distribution of the fluid at the inlet matches the actual working conditions, thus improving the accuracy of the simulation. Its specific geometric parameters are shown in Table 1.



(a) Tapering pipes



(b) Equal cross-section pipes



(c) Gradual Expansion Pipes

Fig. 1. Computational model geometry

Table 1. Specific dimensions of each part of the geometrical model

place	L	H	W	L_f	L_r
lengths (mm)	900	100	200	150	150

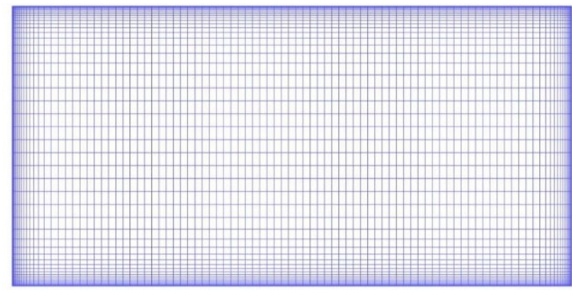


Fig. 2. Pipe XZ direction wall calculation grid

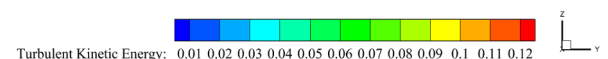
4 Results and discussion

4.1 Characterisation of flow in straight tapering ducts

The inlet velocity in the simulation is three m/s. Since the pipe's TKE and velocity distribution greatly influence particle deposition, the distribution of these two factors in the variable cross-section pipe will be explored. Figures 3 and 4 show the TKE distribution in the variable cross-section pipe, and Figure 5 shows the velocity distribution.



(a) Tapering pipes



(b) Equal cross-section pipes

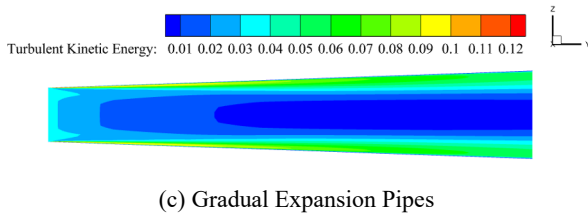


Fig. 3. TKE distribution of YZ section of variable diameter straight pipe at X=100mm

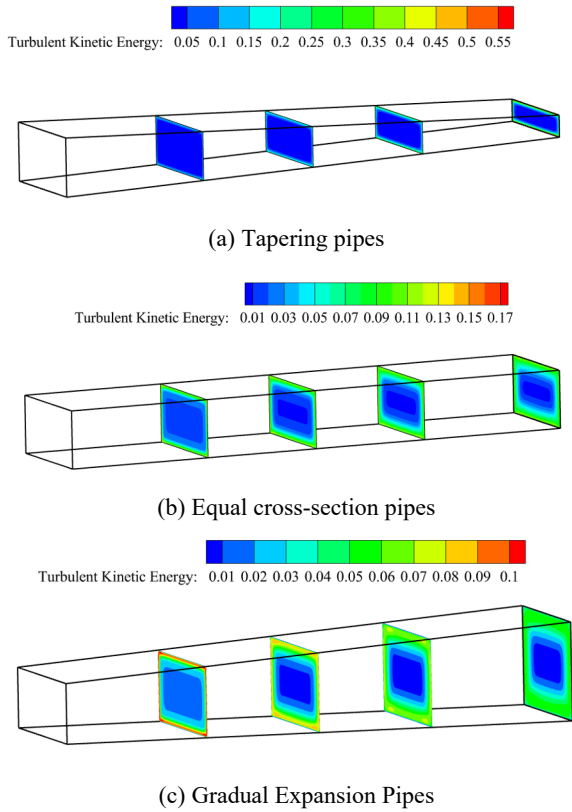


Fig. 4. TKE distribution of XZ section of variable diameter straight pipe

Figures 3 and 4 show the distribution of TKE at different cross sections, from which we can find that the tapering pipe has larger TKE values at the two walls in the Z direction, which is the most obvious at the boundary layer, followed by the equal cross-section pipe. The least apparent TKE maxima appear in the gradual expansion pipe. This indicates that the gradual expansion pipe has the weakest disturbance, the fluid flow is more stable, and the gradient of each variable at the boundary will be smaller than that of the tapering pipe. From Figure 4, it can be found that for the gradual expansion pipe along the flow direction, the TKE distribution of the XZ cross-section varies considerably; the closer to the inlet part of the boundary of the larger TKE, the larger the TKE gradient, which indicates that the closer to the inlet part of the turbulence pulsation is more prominent. For the TKE distribution of the tapering pipe, on the other hand, the closer to the outlet location, the more obvious TKE fluctuation occurs at the boundary of the section.

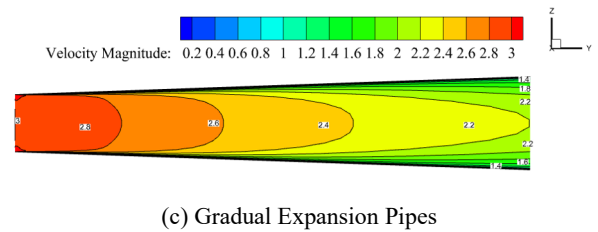
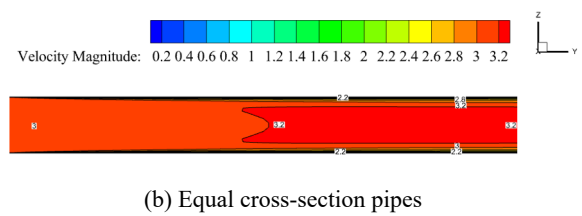
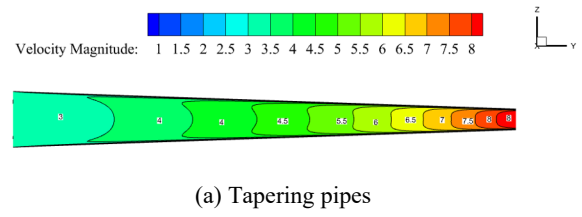


Fig. 5. Velocity cloud of different pipes with YZ section for X=100 mm

Figure 5 shows the velocity distributions of different cross-section types of pipes. The tapering pipe is a nozzle, and the gradual expansion pipe is a diffuser pipe. The velocity distributions obtained from the numerical simulation are consistent with the actual situation, which also verifies the accuracy of this study. The exit velocity of the tapering pipe increases by more than 2.5 times concerning the inlet velocity, and the exit velocity of the gradual expansion pipe decreases by about 26% concerning the inlet velocity.

4.2 Characterisation of particle deposition in straight gradient pipes

Figure 6 shows how the particle deposition efficiency of pipelines with different cross-sections is affected by the change in particle size, from which it can be seen that the particle deposition efficiency of the iso-section pipeline is highest at $d_p \leq 3 \mu m$, followed by the gradual expansion pipe, and the lowest particle deposition efficiency is in the tapered pipeline. This is because the exit velocity of the tapering pipe is more significant, resulting in a decrease in particle deposition efficiency due to small particles being blown directly out of the pipeline or due to resuspension. When the particle size is between 5 and 20 μm , the particle deposition efficiency is highest in the equal cross-section pipe and lowest in the gradual expansion pipe. This is because the role of gravity is gradually manifested as the particle size increases, the gradual expansion pipe gradually becomes taller as the pipeline becomes taller, and the time of particle movement in the direction of gravity increases, leading to a decrease in the number of particles deposited. For the same reason, a tapered pipe has less time for the particles to move in the direction of gravity, and the particles are more straightforward to deposit, partially offsetting the effect

of the higher velocity. When the particle size is between 20 and 50 μm , the particle deposition efficiency growth rate increases faster for the tapered pipe, followed by the gradual expansion pipe, and the lowest particle deposition efficiency is for the equal cross-section pipe. This is because the effect of gravity becomes more critical as the particle size increases. At the same time, the gradual expansion pipe causes the deposition efficiency of large particles to be higher than that of the equal cross-section pipe due to the lower average velocity of the pipe.

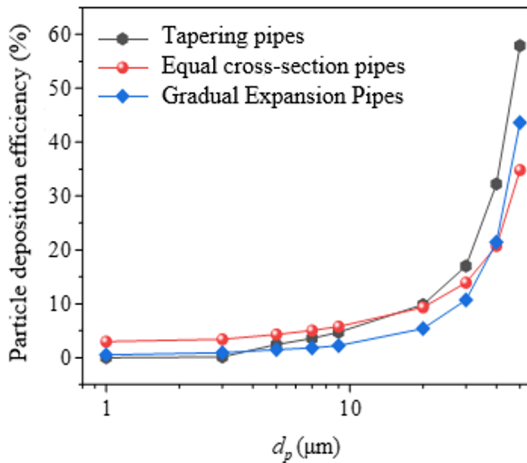
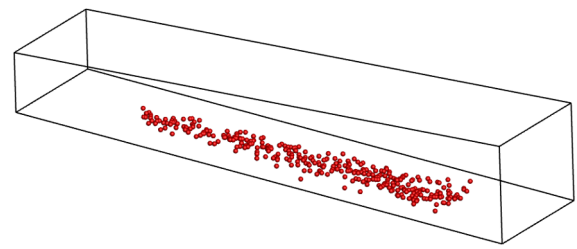
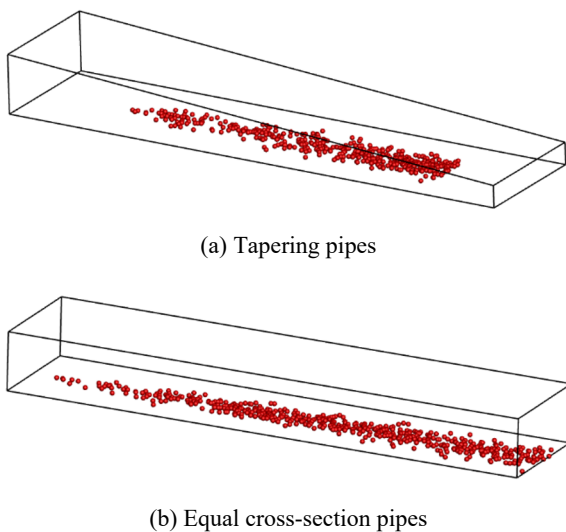


Fig. 6. Deposition efficiency of different particle sizes for pipes of different cross-sections

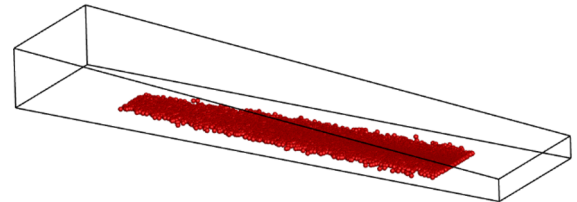
Figures 7 and 8 show the deposition morphology of 5 μm and 50 μm particles in different cross-section pipes to see the particle deposition in more detail. From Figure 7, it can be seen that there is no noticeable difference in the number of particles deposited in different cross-sections of the pipe. The particle deposition gradually increases in the flow direction, and the deposition area gradually becomes more expansive, which is more evident in the two variable cross-section pipes than in the equal cross-section pipe.



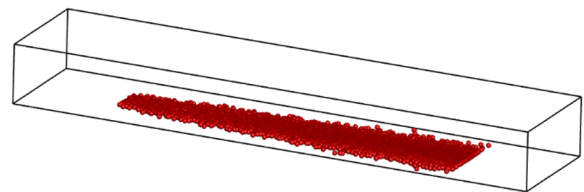
(c) Gradual Expansion Pipes

Fig. 7. Deposition morphology of straight tubes with different cross-sections at a particle size of 5 μm .

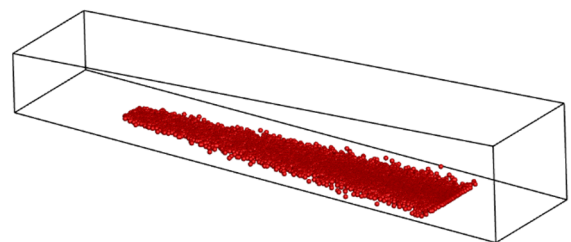
From Figure 8, it can be seen that the width of the particle deposition gradually increases along the flow direction, with the deposition pattern of the gradual expansion pipe near the outlet wider than that of the other pipes, which explains that the particle deposition efficiency of the gradual expansion pipe is higher than that of the equal cross-section pipe as the particles increase. The deposition profiles of the gradual expansion pipe and the equal cross-section pipe are narrower near the inlet, forming an overall sharp trapezoid. In contrast, the average width of the deposition profile of the tapered pipe is more comprehensive, so the tapered pipe has the highest deposition efficiency. Compared to Figure 7, the number of deposited particles is significantly higher, and the accumulation of large particles is more prominent.



(a) Tapering pipes



(b) Equal cross-section pipes



(c) Gradual Expansion Pipes

Fig. 8. Deposition morphology of straight tubes with different cross-sections at a particle size of 50 μm .

5 Conclusions

In this study, the deposition characteristics of coal dust particles in variable cross-section tubes were systematically investigated by numerical simulation, and the following main conclusions were drawn:

(1) Particle deposition efficiency: In the variable cross-section pipe, when the particle size is less than 3 μm , the deposition efficiency of the equal cross-section pipe is the highest, followed by the gradual expansion pipe, and the tapering pipe is the lowest. For particle sizes between 5 and 20 μm , the equal cross-section pipe still had the highest deposition efficiency, and the gradual expansion pipe had the lowest. For particle sizes between 20 and 50 μm , the fastest increase in deposition efficiency was observed in the tapering pipe, followed by the gradual expansion pipe, and the lowest in the equal cross-section pipe.

(2) Detailed analysis of deposition characteristics: It was shown that particle size significantly affects deposition efficiency. Smaller particles were more efficiently deposited in isotropic ducts, while larger particles were more efficiently deposited in conical ducts.

These findings not only deepen the understanding of the deposition characteristics of coal dust particles in boiler tail gas ducts but provide valuable references for practical engineering applications.

Although RSM and DPM models were used in this study, the accuracy and computational efficiency of these models require improvement. Further work should explore more advanced simulation methods and models. Secondly, more experimental studies are necessary to validate the simulation results, and the numerical models should be further optimized and improved by calibrating the experimental data to better reflect the actual working conditions.

The authors appreciate the financial support provided by the Xinjiang Major Science and Technology Special Project (No.2022A01002-2), the National Key Research and Development Program of China (No.2023YFB4102704), the Xinjiang Regional Coordination Special Project-International Science and Technology Cooperation Program (No.2022E01026).

References

1. W. Gang, D. Jianguo, Z. Ying, Z. Qiang. Air pollutant emissions from coal-fired power plants in China over the past two decades [J]. *Sci. Total Environ*, **741**, 140326 (2020).
2. W. Jianmin, W. Lixiang, W Han. Study on the impact of reducing fossil energy use on China's existing economic structure under carbon neutrality goals [J]. *J. Cleaner Prod*, **449**, 141819 (2024).
3. C. Wei , M. Yanchun, Y. Rudai. Regional Economic Growth, Energy Consumption Structure and Carbon Neutrality in China [J]. *Consumer Economics*, **39**, 5 (2023).
4. J. Zhijun, Z. Chuan. Thinking about China's Energy Transition Path towards Carbon Neutrality [J]. *Journal of Peking University (Natural Science Edition)*: 1-9.
5. D. Tayebbeh, R. Mikael, W. Lars. Effect of operation conditions on particulate matter removal by a packed-bed wet scrubber for a small-scale biofuel boiler [J]. *Therm. Sci. Eng. Prog*, **47**, 102290 (2024).
6. L. Xiangdong, Y. Yihuan, S. Yidan, T. Jiyuan. An Eulerian–Eulerian model for particulate matter transport in indoor spaces [J]. *Build Environ*, **86** (2015).
7. J. Hai, L. Lin, S. Ke. Simulation of particle deposition in ventilation duct with a particle–wall impact model [J]. *Build Environ*, **45**, 5 (2010).
8. X. Zhiming, H. Zhimin, Q. Hongwei. Comparison between Lagrangian and Eulerian approaches for prediction of particle deposition in turbulent flows [J]. *Powder Technol*, **360** (2020).
9. Y. Jingxin, Y. Yao, H. Zhengliang. Impact of viscosity model on simulation of condensed particle flow by Euler multiphase flow model [J]. *CIESC J*, **71**, 11 (2020).
10. L. Hao, L. Liu, J. Yu. Numerical study of monodispersed particle deposition rates in variable-section ducts with different expanding or contracting ratios [J]. *Appl. Therm. Eng*, **110** (2017).
11. Y. Xin, I. Derek, M. Lin. Understanding the ash deposition formation in Zhundong lignite combustion through dynamic CFD modelling analysis [J]. *FUEL*, **194** (2017).
12. H. Zhimin, X. Zhiming, Y. Xiaoyan. CFD modeling for prediction of particulate fouling of heat transfer surface in turbulent flow [J]. *Int. J. Heat Mass Transfer*, Dec, **144** (2019).
13. T. Lin, A. Goodarz. Particle deposition in turbulent duct flows—comparisons of different model predictions [J]. *J. Aerosol Sci*, **38**, 4 (2007).
14. X. Xiaoyang, L. Yunhao, Z. Houjian. Turbulence statistics analysis of cross flow and heat transfer over an inline tube bundle using DNS [J]. *Int. J. Heat Fluid Flow*, **107** (2024).
15. V. Francisco, C. Jeff L, C. Walter G. On the Development of an Asphaltene Deposition Simulator [J]. *Energy Fuels*, **24**, 4 (2010).
16. M.M.Gibson, B.E.Launder. Ground effects on pressure fluctuations in the atmospheric boundary layer [J]. *J. Fluid Mech*, **86** (1987).
17. T. Lin, A. Goodarz. Particle deposition in turbulent duct flows—Comparisons of different model predictions [J]. *J. Aerosol Sci*, **38**, 4 (2007).
18. H. Aodi, Y. Xiaoyan. The deposition characteristics of micron particles in heat exchange pipelines [J]. *Appl. Therm. Eng: Design, processes, equipment, economics*, **158** (2019).